Agent-Based Simulation of Building Evacuation after an Earthquake: Coupling Human Behavior with Structural Response

Z. Liu[1]; C. C. Jacques, S.M.ASCE[2]; S. Szyniszewski, Ph.D.[3]; J. K. Guest, Ph.D., A.M.ASCE[4]; B. W. Schafer, Ph.D., P.E., A.M.ASCE[5]; T. Igusa, Ph.D.[6]; and J. Mitrani-Reiser, Ph.D., A.M.ASCE[7]

Abstract: The safety of building occupants during and immediately after disasters, such as a major earthquake, is highly dependent on the way in which people interact with the damaged physical environment. While there are extensive studies on evacuation from undamaged structures and on structural behavior under seismic and other hazards, research on the influence of building damage on human evacuation behavior is limited. This study presents a framework by which models for buildings and human behavior can be coupled to analyze the dynamic influences of building damage on the evacuation process. The framework combines nonlinear dynamic finite-element modeling of structures, probabilistic modeling of damage, and agent-based modeling of human occupants to investigate the behavior of people as they interact with each other and with their dynamically-deteriorating environment as they attempt to evacuate the building. A case study is presented for a typical three-story commercial office building subjected to the ground motions of the 1994 Northridge, California earthquake. By using exit flow rates and other measures related to evacuation time histories as the outcomes of interest, it is shown how the proposed framework can be used as a tool to enhance building design and to develop recommendations for improved evacuation strategies. An important future extension of the work is expanding the framework for multiple buildings for community-wide models of postdisaster behavior.
DOI: 10.1061/(ASCE)NH.1527-6996.0000199.

Introduction

The study of evacuation behavior from damaged structures plays an important role in preparedness for seismic disasters including deployment of first responders and distribution of supplies (Fiedrich et al. 2000). Evacuation models can inform casualty models, which depend upon an understanding of how occupants are impacted by hazards that threaten the built environment (Coburm et al. 1992). However, data on building evacuation are rarely recorded during actual seismic events. Therefore, to develop a realistic understanding of evacuation processes after an earthquake, it is necessary to develop a simulation method that realistically combines existing knowledge on building evacuations with engineering expertise in seismic impacts on the built environment. This study proposes a computational-based framework for modeling evacuations in buildings and demonstrates the use of this framework on a building case study.

[1]Ph.D. Candidate, Dept. of Civil Engineering, Johns Hopkins Univ., Baltimore, MD 21218. E-mail: zliu36@jhu.edu

[2]Ph.D. Candidate, Dept. of Civil Engineering, Johns Hopkins Univ., Baltimore, MD 21218. E-mail: cjaque2@jhu.edu

[3]Lecturer, Dept. of Civil and Environmental Engineering, Univ. of Surrey, Guildford, Surrey GU2 7XH, U.K. E-mail: s.szyniszewski@surrey.ac.uk

[4]Associate Professor, Dept. of Civil Engineering, Johns Hopkins Univ., Baltimore, MD 21218. E-mail: jguest4@jhu.edu

[5]Professor, Dept. of Civil Engineering, Johns Hopkins Univ., Baltimore, MD 21218. E-mail: schafer@jhu.edu

[6]Professor, Dept. of Civil Engineering, Johns Hopkins Univ., Baltimore, MD 21218. E-mail: tigusa@jhu.edu

[7]Assistant Professor, Dept. of Civil Engineering, Johns Hopkins Univ., Baltimore, MD 21218 (corresponding author). E-mail: jmitrani@jhu.edu

Note. This manuscript was submitted on December 8, 2014; approved on August 14, 2015; published online on October 29, 2015. Discussion period open until March 29, 2016; separate discussions must be submitted for individual papers. This paper is part of the ***Natural Hazards Review***, © ASCE, ISSN 1527-6988.

Background

Evacuation patterns and behaviors have been studied extensively by researchers from a wide range of disciplines. However, nearly all qualitative studies that have been performed are based on observations of humans evacuating in so-called drill situations where buildings are undamaged and participants are responding to a simulated emergency. Since there is no true danger in the simulation, the participants are able to behave calmly, without behaviors such as pushing or rushing that may occur under dangerous conditions (Hostikka et al. 2007; Peacock et al. 2010). Studies of evacuations that occurred in true disaster scenarios are performed retrospectively, relying upon the memory of evacuees for information on the evacuation process (Horiuchi et al. 1986; Galea et al. 2007). It has not been possible to obtain detailed quantitative data on evacuation processes and human behavior during evacuations in true disaster scenarios, though methods for doing so have been proposed (Gwynne 2013).

To address this data gap, many researchers have turned to computational simulation and modeling to provide a better understanding of evacuation. Based on how the space is modeled, these models can be classified into continuous models and discrete models. Social force models are typical continuous models. In those models, pedestrians are modeled as particles with certain mass and size, and by solving the acceleration equation with some virtual social forces, such as attraction force, repulsive interaction force, body force, sliding friction force, and fluctuation, the particles' positions can be determined. The most important social force model is Helbing's models (Helbing and Molnar 1995, 2000), in which pedestrian crowds in both normal and panic situations are modeled and to observe evacuation phenomenon, such as clogging, lane forming and the fast-is-slower effect. However, Still (2000) highlights that these social-force models contradict with the basic fact that human beings have their own choice of direction and can stop and start at will. Cellular automaton (CA) models (Dijkstra et al. 2000; Kirchner and Schadschneider 2002; AEA-Technology 2002) are typical discrete models. In a CA model, the evacuation area is discretized as uniform 2D lattices or cells with one or more variables. Each cell can be empty or occupied by an obstacle, pedestrian, or group of pedestrians. A pedestrian can move to an empty neighboring cell at each time step based on a set of local rules. Most discrete models can be thought of as mutations of CA models, such as EXODUS (Galea and Perez Galparsoro 1994), in which the evacuation surface is discretized as node-arc topology and pedestrians travel between nodes through the arcs. Those discrete models provide realistic results when crowd density is medium or low, but have unrealistic results in high-density situations. Besides, social behaviors among pedestrians are usually ignored. These models focus on modeling individual behavior and interaction with others, thus they are classified as microscopic models. The models that focus on the system as a whole, rather than the individuals, are considered to be macroscopic. Macroscopic models, i.e., fluid or gas kinetic models (Henderson 1971; Helbing 1992; Hughes 2000), assume that pedestrians, as one homogenous population, behave like a fluid or gas, respectively. In these models, partial equations governing the gas or fluid dynamics are used to describe how the crowd density and velocity change with time and space. Although these models can capture features of the whole system accurately, they fail to reflect individual behaviors and decision mechanisms; they are also limited to fairly simple geometries.

Agent-based modeling (ABM) is one computational technique that can model the behavior of large numbers of interacting individuals. While the algorithms of ABMs operate primarily at the individual level, the interactions between these individuals can generate significantly different, and even unexpected, mass response (Epstein 1996, 1999). A wide variety of studies have utilized this technique to examine the human aspects of evacuation. Zarboutis and Marmaras (2004) studied the evacuation of a metro tunnel and found significant sensitivity with respect to choices made by the train driver and passengers. Pan (2006) modeled the evacuation of a multistory university building that accounted for a wide variety of crowd behaviors, including competition, queuing, herding, and altruism. Chu et al. (2014) developed an egress simulation tool, *SAFEgress*, which incorporates several important collective behaviors such as grouping and herding.

The present paper extends these ABM studies by incorporating engineering models of the structural hazards faced by evacuees in their physical environment. Additionally, novel algorithms are presented for modeling individualistic and collective behaviors in seismic evacuation scenarios. This paper presents the methodologies used to simulate the structural response to earthquakes, the subsequent damage and casualty/injury analyses, and the evacuation simulation. The results of simulated evacuations from a low-rise commercial building are also provided. Finally, the last section provides some conclusions from the presented work and identifies some important future directions for the work.

Methods

To create realistic simulations of the evacuation of a building damaged by a seismic event, a high-fidelity physics-based model of the response of the built environment must be combined with detailed human behavioral modeling in a manner that captures the interactions between the building and its occupants. The proposed framework accomplishes this through the use of three main submodels: a nonlinear dynamic finite-element model to determine the response of the structure; a probabilistic damage and loss assessment model to assess building impacts and occupant injuries; and an agent-based model to capture individual and collective behavior of occupants immediately after shaking subsides. These submodels and their couplings are described in the following three subsections.

Structural Damage Modeling

To model the dynamic response of a structure under extreme seismic loading, the following requirements must be satisfied. Nonlinearities due to large strains and large displacements must be included to account for material yielding and member buckling, as well as methods to capture elements that detach and fall away from the structure as collapse occurs. Since the properties of beam–column joints in frame structures typically play a significant role in building response, it becomes necessary to model these connections in detail rather than simply idealizing them as rigid or pinned connections.

This work uses *LS-DYNA* (Wilensky 1999), a multiphysics simulation software package developed at the Lawrence Livermore National Laboratory, which contains tools suitable for addressing all of these modeling requirements. Hughes-Liu beam elements (Hughes and Liu 1981a, b) allow for cases where both large displacements and large strains are present, since they are incrementally objective (i.e., rigid body rotations do not generate strains). Several material models are available to capture various assumptions on constitutive behavior. Material number 24, referred to as Piecewise Linear Isotropic Plasticity, for example, models elastic-plastic behavior in metallic materials and is a suitable choice for modeling the behavior of steel under large strains. *LS-DYNA* can also model material failure by calculating the plastic strain across multiple integration points in an element, and deleting that element when the strain exceeds a user-prescribed critical value (Hallquist 2006). Beam–column connections are modeled as nonlinear spring elements, which have been calibrated through high-resolution simulations performed by Lim and Krauthammer (2006). This representation of connections is computationally efficient, and closely matches alternative macromodeling methods (Khandelwal et al. 2008; Sadek et al. 2011).

By subjecting a structure to a seismic ground motion and performing a dynamic, non-linear finite-element analysis of its response in *LS-DYNA*, it is possible to estimate overall structural damage, including both partial or total collapse, as well as a wide variety of other engineering demand parameters.

Probabilistic Non-Structural Damage and Injury Modeling

While finite-element modeling is highly suitable for capturing structural damage such as column failure and progressive collapse of slabs, it is less suitable for capturing damage to nonstructural elements such as cracking of partition walls or sagging of suspended ceilings. It is, however, still possible to use the results of the structural model to determine nonstructural damage. The deterministic finite-element model of the structure can be used to inform a probabilistic damage assessment of the nonstructural building components (Mitrani-Reiser and Beck 2007), which can significantly hinder human movement throughout the building in an evacuation.

The first step in the nonstructural damage modeling is to create a detailed nonstructural inventory from existing building drawings. It

Nat. Hazards Rev., 2016, 17(1): 04015019

is assumed that certain components (i.e., suspended ceiling tiles) are equally distributed throughout a building, with nominal properties based on the building's size and its occupancy type. Next, the fragility functions are gathered from existing literature and databases [e.g., ATC-58 (ATC 2012)]. A fragility function defines the probability that damage to a component exceeds a particular damage state conditioned on a given value of structural response, x, provided by the structural analysis. The structural response can be described by a number of engineering demand parameters, such as peak floor accelerations or peak interstory drift ratios. Many fragility functions are formulated assuming that the probability of damage follows a lognormal distribution, which is consistent with the observed failure of many structural and nonstructural components (Beck et al. 2002; Krawinkler 2005; Pagni and Lowes 2006; Badillo-Almaraz et al. 2007). The form of these idealized fragility functions for each damage state, d, is then described by

$$F_{X_d}(x) = \Phi\left[\frac{\ln(x/x_m)}{\beta}\right] \tag{1}$$

where X_d = component's capacity to resist damage state d; x_m = median capacity for damage state d; and β = logarithmic standard deviation. The structural response parameter, x, is determined directly as output from the structural model.

Each individual component may have multiple damage states. These damage states are denoted as $D \in \{0, 1, 2, \ldots, m\}$, where m is the total number of possible damage states, and a state of $D = 0$ indicates that the building component is undamaged. These damage states are generally assumed to be both progressive and mutually exclusive. Under these assumptions, the probabilities of an individual component being in each possible damage state are described by

$$P[D = d|x] = \begin{cases} 1 - F_{X_1}(x) & d = 0 \\ F_{X_d}(x) - F_{X_{d+1}}(x) & 1 \le d \le m-1 \\ F_{X_m}(x) & d = m \end{cases} \tag{2}$$

given by Porter et al. (2007). With the inventory of nonstructural components and the associated fragility functions, the results from the nonlinear structural analysis can then used to assess the probabilities of being in each damage state. Given the deterministic structural-analysis results, Monte Carlo simulations (MCS) are performed to assess the uncertainty in evacuation times based on variability of damaged means of egress caused by fallen debris during strong ground shaking and of agent behaviors (described in the following section). The damage for each nonstructural component in the structure can be determined from Eq. (2) using an inverse method. That is, let $P[D = d|x] = U$, where U is a uniformly-distributed random variable falling with the interval [0,1]. The damage state for the given component can be solved from Eq. (2). Then damage states for all nonstructural components are determined by repeating this procedure.

Before the start of the simulation, the agents in the model are designated as being in one of four health states: healthy, minor injuries, major injuries, or death. The probabilities for these health states can be determined directly from the structural and damage analyses (Mitrani-Reiser and Beck 2007; ATC 2012) when empirical data of fatality rates for specific building types are available. However, since fatality rates were not available for the study building, the initial probabilities for the agent's health states in the simulations were determined from the ATC-13 (Applied Technology Council 1985) report on data for the estimation of earthquake loss in California. This report provides probabilities of each of the health states conditioned on building damage states. The health states of individuals in the building impact their mobility, and thus evacuation speed. The probabilities of health states were modified for the study building to account for the alteration of the structural system (making it non-code-compliant in the damaged scenario); these modifications induce more damage and subsequently more-complex dynamic human behavior in an evacuation.

Agent-Based Human Behavioral Modeling

The human behavioral module of the proposed framework incorporates a realistic heterogeneous population of building occupants who can individually navigate through a damaged environment and engage in a variety of social behaviors that are related to the evacuation process. This module also captures important data, such as evacuation time histories and flow rates throughout the building. The agent-based modeling platform *NetLogo* (Wilensky 2010) is used to model human evacuation after an earthquake under undamaged and damaged conditions.

Creating the Built Environment

The nonstructural layout of the building is imported into *NetLogo* through a set of color-coded image files (Fig. 1) to create the environment for the ABM. The environment consists of a rectangular grid of square patches that store data about the physical features of the environment (e.g., doors, walls, hallways, rooms, and staircases) and associated damage states. Results from the damage

Fig. 1. (Color) The floor plans for the (a) ground floor; (b) upper stories, showing the locations of walls (purple), doors (red), windows (blue), exits (green), stairs (yellow) and elevators (brown)

Table 1. Summary of Agent Characteristics, Where the Values in Parentheses Are the Actual Speeds Used in the Model

Age group	Gender	Body radius (m)	Speed (m/s)		Step frequency (steps/s) in model		Stride (m) in model	
			Flat	Stairs	Flat	Stairs	Flat	Stairs
Young adult[a]	Female	0.24 ± 0.02	1.45(1.42)	0.65(0.66)	2	1	0.71	0.66
	Male	0.27 ± 0.02	1.48(1.52)	0.81(0.81)	2	1	0.76	0.81
Old adult[b]	Female	0.25 ± 0.02	0.93(0.91)	0.56(0.56)	2	1	0.46	0.56
	Male	0.25 ± 0.02	1.06(1.12)	0.60(0.61)	2	1	0.56	0.61

[a]Adult aged 20–31, based on the study in Laufer (2003).
[b]Adult aged 65–89 based on the study in Laufer (2003).

assessment are imported into the space as a property of these patches. In places within the ABM environment that should be passable (i.e., hallway) but where damage is sufficiently severe to prevent egress, the patch is designated as an obstacle similar to permanent obstacles (i.e., a wall) in the ABM environment. In places that ought to be passable but where the damage is moderate, the patch will be designated as damaged, which impacts egress with an assumed reduction in travel velocity of agents in through these sections. The current version of the agent-based model does not allow for cases where all means of egress are compromised, though future development of the framework could easily be adapted to account for this severe condition. Since the dimensions of each floor are identical in the study building, the data for all floors can be overlaid on the same patch for computation efficiency. However, agents can only use the information for the floor on which they are currently located. As in the case for actual buildings, exit signs are included in the model to facilitate navigation for agents unfamiliar with the building.

Creating the Agents

Building occupancy is determined by the square footage and population rates for the occupancy type of the study building [i.e., as in ATC-13 (ATC 1985)], which results in an average number of people per square foot for a standard commercial building. This number can be taken as the baseline population for the study structure, and can then be scaled up or down to account for underpopulation or overpopulation.

Each human in the model is then represented by a square agent. The square shape was chosen for its ability to simulate high density crowds, as described in Still (2000), as well as for its compatibility with the *NetLogo* modeling platform. Each of these agents is assigned an age group (i.e., young adult or old adult, as defined in Laufer 2003) and a gender (i.e., male or female). Based on the case study in Gwynne and Boswell (2009) for an office building, two-thirds of the population are assigned to be young adults, and one-third to be old adults; 44% are male and 56% are female. Children are not included in the current model because the study building is assumed to be an office building. Each agent's age and gender are used to assign a body size, based on information in Hostikka et al. (2007), as well as a walking speed, stride length, and step frequency based on data described in Laufer (2003) for flat surfaces and Fruin (1971) for stairs with a 27° gradient. For each MCS, each agent in the building is assigned an altruism constant C_p, sampled from a normal distribution with a user-selected mean (0.8) and standard deviation (0.05). A high C_p constant indicates a high tendency towards altruistic behaviors, as described in the next subsection. Since the simulation updates every second, step frequencies for flat surfaces are determined by rounding the values provided by Laufer (2003) to the nearest whole steps per second. Preliminary ABM simulations results by the authors indicated that restricting people's step frequencies on stairs provides more realistic results than restricting their stride lengths by the height of the stair tread; this is because stairs are modeled as 2D incline surfaces in the model. Thus, step frequencies in stairs are determined by step frequencies on flat surfaces multiplied by the ratio of flat-surface speeds to stair-surface speeds and rounded to the nearest whole steps. Stride lengths are determined by speeds divided by step frequencies, rounded to the nearest integer. A summary of these basic agent characteristics is provided in Table 1. Injuries can also affect the speed of an agent; agents who suffer either minor or major injuries are assumed to have their maximum speed reduced to 75 and 10% of their original speeds, respectively. In addition, the severely-injured agents' step frequencies are reduced to 1 step per second to reflect a decrease in their agility.

Navigating the Space

The new navigation algorithm developed for this study is designed to allow agents to take realistically-sized steps in space without passing through objects or other people and can take multiple steps in each increment of time in the model. To simulate spontaneity, agents are not constrained to synchronize their steps with the steps of other agents or with the time increments in the model.

Each agent is programmed to navigate the space by choosing a path in the direction of their desired evacuation goal while avoiding obstacles and other agents along the way. The navigation is facilitated by using an initial feasible destination region, P_{m0}, shown in Fig. 2 that is a circular area with a radius equal to the agent's stride length. However, before deciding the direction of their next step, each agent examines the space around them with a radius determined by their stride length plus one half the maximum body size

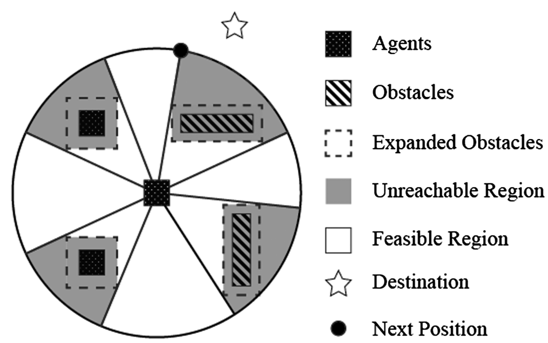

Fig. 2. Example search of the feasible destination region for an agent centered at the origin; dotted pattern represents patches for agents, and the hatched pattern represents patches with obstacles; dashed lines represent the expanded outline of obstacles and agents; shaded grey designates the unreachable region, and the white represents the final feasible region P_m; star represents the center agent's evacuation target and the solid dot shows the agent's next position

of all agents. When this disk is empty of obstacles and other agents, then the true feasible region, P_m, is equal to P_{m0}. If there are obstacles in the space around the agent, then parts of P_{m0} are actually unreachable, and must be excluded from P_m. The definition of P_m is then the set of all patches of P_{m0} that are not in the unreachable set, also shown in Fig. 2.

To find the unreachable region, first the obstacles are enlarged by one-half of the agent's body size, indicated by dashed lines in Fig. 2, to avoid agents colliding with obstacles. Next, to ensure that the agent does not try to pass through any obstacles, the agent uses tangent lines to locate the boundaries of the region that is behind the expanded obstacle from the agent's point of view. Then any area enclosed by an expanded obstacle's border and the tangent lines to this obstacle is an unreachable area, shown as the shaded grey zones in Fig. 2; these areas are subsequently removed from P_{m0}. The same process is repeated for all obstacles in the disk, leaving the white zones as the final feasible region P_m. If P_m is not null, the agent will move to a patch in P_m closest to its destination. In Fig. 2, the agent at the center will choose to take a step towards the solid black dot, which gets them closest to the designation (the star) while avoiding the areas occupied by other agents and obstacles (the shaded grey regions).

Various search-space representations, such as grids, waypoint graphs, and navigation meshes can be used to guide an agent in finding the shortest path to their destination. Grids are straightforward and represent the environment as patches that are either passable or impassible, but are unlikely to find optimal paths from one point to another in the building. Waypoint graphs use nodes and lines to represent ways that are safe for traversing, but can result in path-finding artifacts, such as unnecessary zigzagging. Navigation meshes support more intelligent decision-making in path finding and are a combination of grids and waypoint graphs; they describe the areas where agents can safely traverse without crossing the edges of the polygon. The model in this study uses a navigation mesh, which subdivides each floor into many convex polygons of passable space, where each adjoining polygon shares two points and an edge, and no two polygons overlap. Waypoints are assigned to the vertices and edges of the polygons, simplifying path-finding of all agents within a finite graph.

Agents who are familiar with the building may choose their destinations based on their preferences or daily habits. For example, in the case study agents on the upper floors are assumed to select the closest staircase from their location as their destination, then go through the staircase and finally evacuate from a side exit closest to the staircase. For agents on the first floor, it is assumed that they will choose the main exit as their destination unless they are on polygons adjacent to the side exits. If an agent discovers that a destination is no longer viable due to excessive damage, then they will choose another destination instead.

The destination-seeking process is performed dynamically for agents unfamiliar with the building, using updates based on observations from their environment. The agents will start by searching a circular sector in front of them with a user-selected radius (the visual radius) and an angle equal to 120°, the average range of human vision (Stidwill and Fletcher 2010). The method to determine an agent's visible region is the same as the method to determine the feasible region, except other agents are not considered as obstacles, and the edge of the obstacles are not expanded by half of the agent's body size. If agents find other people in their visible region (the circular sector), they will consider the destination path of these other agents and adopt the destination of the plurality. Otherwise, individual agents will try to locate a destination on their own by following a set of five simple rules. The first rule governs the behavior of agents in a room or internal corridor. If inside a room that has a door, agents will set their destination to be that door and attempt to exit through it. If the room has no door, but agents find an exit sign, they will face the direction indicated on the sign and search again. If there is no door or sign, they will move randomly. The agents retain the memory of the rooms they have already visited. The second rule governs the behavior of agents in main corridors on upper stories. Agents that are in corridors will follow the same steps as those in rooms, but will prioritize staircases over doors. The third rule governs the behavior of agents in the main corridors of the ground floor; this rule is identical to the second rule except that agents on the ground floor prioritize external exits rather than staircases. The fourth rule governs the behavior of agents in staircases, where agents descend until they reach the first floor and proceed to exit the staircase. Agents also follow a fifth and final rule which is simply to avoid rooms or corridors that they have already been checked and have no suitable exits.

Determining Social Interactions

Agents choose whether to engage in collective and social behaviors in the model based on their personal characteristics, input from their environment, and interactions with other agents. Four types of collective and social algorithms are included in the egress model: grouping, herding, rescuing, and information sharing. Helbing et al. (2000), Pan (2006), and Chu et al. (2014) describe grouping and herding behavior in real and simulated evacuations. Horiuchi et al. (1986) observed rescuing behavior in a fire evacuation of an office building in Osaka, Japan, and Peacock et al. (2013) and Johnson (2005) note that rescuing behavior were observed in the World Trade Center evacuations, and have been seen in other events as well.

Agents encountering those with whom they share social relationships trigger the grouping in this model. Social relationships, such as coworkers in the same office or firm, are determined in the model by each agent's unique home-base identifier. Agents who share the same home base are assumed to share a strong social relationship. Agents whose home bases are close to each other are also assumed to share a social relationship, but these relationships are less strong. Only agents who are familiar with the building are assigned a home base, and only these agents who are familiar with the building can engage in grouping behavior directly. When agent i, who is capable of grouping, is not in a group and encounters other agents who are capable of grouping, they first identify the closest of these other agents (agent j). Then, agent i will calculate the probability of forming a group with agent j based on their willingness to group with strangers (using distance as a proxy) and their willingness to group with people they know (using a ratio of their home-base identifiers as a proxy for the strength of their social connection), according to the following:

$$P[\text{grouping}_{ij}] = \begin{cases} (1-w)\cdot f(d) + w\cdot\left(1-\frac{|b_i-b_j|}{B}\right) & \text{for } |b_i-b_j|\leq B \\ (1-w)\cdot f(d) & \text{for } |b_i-b_j|>B \end{cases}$$

$$f(d) = \begin{cases} 1 & \text{for } d\leq s \\ e^{(s-d)/s} & \text{for } d>s \end{cases} \tag{3}$$

where $w \in [0,1]$ = user-defined importance of social interactions; b_i and b_j = home-base identifiers of agents i and j, respectively; B = user-defined constant, which represents the maximum difference of the group number for any pair of evacuees who are considered to have a social relationship; d = distance between agents i and j; and s = distance agent i can travel in one second. To determine if a group actually forms, a random number between 0 and 1 is generated, and if that random number is less than $P[\text{grouping}_{ij}]$, agent i will group with agent j. Once the decision to form a group is

Nat. Hazards Rev., 2016, 17(1): 04015019

made, agent i sets its group to be the set of agent j and any other agents with whom agent j shares a group. All of the other agents in this newly-enlarged group adds agent i as a new group-mate.

An agent may switch groups if the agent is currently grouped with people with whom it shares a weak social bond and encounters a group with whom it shares a significantly stronger social bond. To determine whether the agent will switch, agent i first calculates $P[\text{grouping}_{ij}]$ for the agent j, who has the median grouping number of its current group, and $P[\text{grouping}_{ik}]$ for agent k, who has the median grouping number of the potential new group. $P[\text{grouping}_{ik}]$ is then scaled by D_c, which is a factor less than or equal to one, to quantify the natural aversion to switch groups. Then the probability of switching groups is calculated as

$$P[\text{switch}] = P[\text{grouping}_{ik}] \times D_c - P[\text{grouping}_{ij}] \tag{4}$$

To determine if agent i switches groups, a random number between 0 and 1 is generated, and if that random number is less than $P[\text{switch}]$, agent i will switch to the group with agent k. Once the decision to switch groups is made, agent i is removed from the group set of the members of the current group, empties its own group set, then joins the new group following the steps previously listed.

Grouping behavior has two main stages: gathering and traveling. During the gathering phase, an agent finds the center of mass of their visible group mates from its point of view, and moves towards that center of mass until the agent is within a group radius, R_g, of that center of mass. The group radius is determined as follows:

$$R_g = c \cdot A_v \cdot L_m \tag{5}$$

where A_v = number of agents in a 60° circular sector with the agent at the midpoint of the arc of the sector; L_m = maximum diameter of the agents in that circular sector; and c = constant which is set as 1.1. Agents within a group are considered gathered once they are within the group radius and then switch to the traveling mode. In traveling mode, the agent moves towards the destination held by the plurality of the group members. If more than one destination is held by a plurality, one of these destinations is randomly selected to be the group destination. In traveling mode, all members of the group set their velocity to that of their slowest group-mate, as is consistent with the behavior described by Proulx and McQueen (1994).

The herding algorithm in this model is reserved for agents who are unfamiliar with the building. Their lack of knowledge of the evacuation pathways of the building may induce a high degree of stress (Pelechano and Malkawi 2008), which is strongly correlated with following the crowd (Helbing et al. 2000; Pan 2006). The way in which agents in the model who do not know the building layout adopt this behavior is described previously; such an agent simply adopt the destination held by most of the agents in its field of vision.

Rescuing and information sharing allow agents to behave altruistically. Information sharing allows agents to assist others by telling them about waypoints that are no longer passable, so agents can switch to secondary destinations without personally observing the damage. Agents who have knowledge on newly-impassable waypoints can share this information with agents they encounter that do not know about the status of that waypoint if their altruism constant C_p is greater than a generated random number in [0,0.6]. Rescuing allows agents to help each other by increasing the mobility of injured agents. When a healthy (or mildly injured) agent i who is not already rescuing someone encounters an injured (or more-severely injured) agent j who is not currently being rescued, the healthy agent calculates the probability of rescuing in one of two ways. If the healthy agent and the injured agent are both not familiar with the building, then the healthy agent's probability of rescuing is simply equal to its altruism constant C_p. If both agents are familiar with the building, however, then the healthy agent calculates its willingness to rescue using the following:

$$P[\text{rescue}_{ij}] = C_{Pi}\left(1 + \frac{0.5}{1 + |b_i - b_j|}\right) \tag{6}$$

where, b_i and b_j are home-base identifiers defined as in Eq. (3). Again, a random number between 0 and 1 is generated, and if that random number is less than $P[\text{rescue}_{ij}]$, agent i will choose to rescue agent j. Once the decision to rescue has been made, agents i and j will move together for the rest of the simulation. They will essentially act as one agent with a larger body size, and are assumed to move at half of agent i's normal walking speed. They can still participate in grouping or herding with their combined knowledge level and with agent i's social characteristics.

Case Study

To illustrate the evacuation simulation framework, a case study of an archetypical three-story, densely occupied office building is examined in detail. The case study, which forcibly damages a vertical means of egress in the damaged scenario, is inspired by complications of evacuating occupants in the Christchurch, New Zealand earthquake on February 22, 2011, due to the failures of staircases.

Analyzing the Archetypical Building

A low-rise steel moment–frame structure originally described in Gupta and Krawinkler (2000) and further studied in Foley et al. (2008) was used as the study building. This structure, shown in Fig. 3, consists of three identical stories with a 6 × 4-bay footprint and two staircases located in the northeast and southwest corners. It is designed to comply with standard United States' requirements for dead, live, wind, and seismic loads. The original design is used as a baseline structure in the evacuation model and an altered (non-code-compliant) structural design is used as the damaged structure in the evacuation model. In the altered design, the exterior moment-resisting frames were moved to the interior of the building, disrupting the symmetry of the building, and thereby making the structure susceptible to increased torsional loads.

Nonstructural Layouts

To create a realistic damaged environment for the evacuating agents in the simulations, the case-study building was populated with typical nonstructural components. The floor plans for all stories were developed using the Los Angeles Municipal Code (LAMC 2013) and empirical data of office buildings in the United States. The first of these floor plans, shown in Fig. 1(a), represents the ground floor, which includes several offices connected by various corridors. The large entrance on the south end of the building serves as the primary exit, while smaller fire doors at the southwest and northeast corners service the staircases at those same locations. The building also includes a main elevator shaft near its center, though this was not used in the simulations because occupants are discouraged from using elevators after an earthquake. The second floor plan, shown in Fig. 1(b), represents the layout of the second and third floors of the study building. Like the first floor, it consisted of several offices connected by large main corridors. Unlike the first floor, it has no exterior exits, and can only be accessed via the two staircases or the elevator.

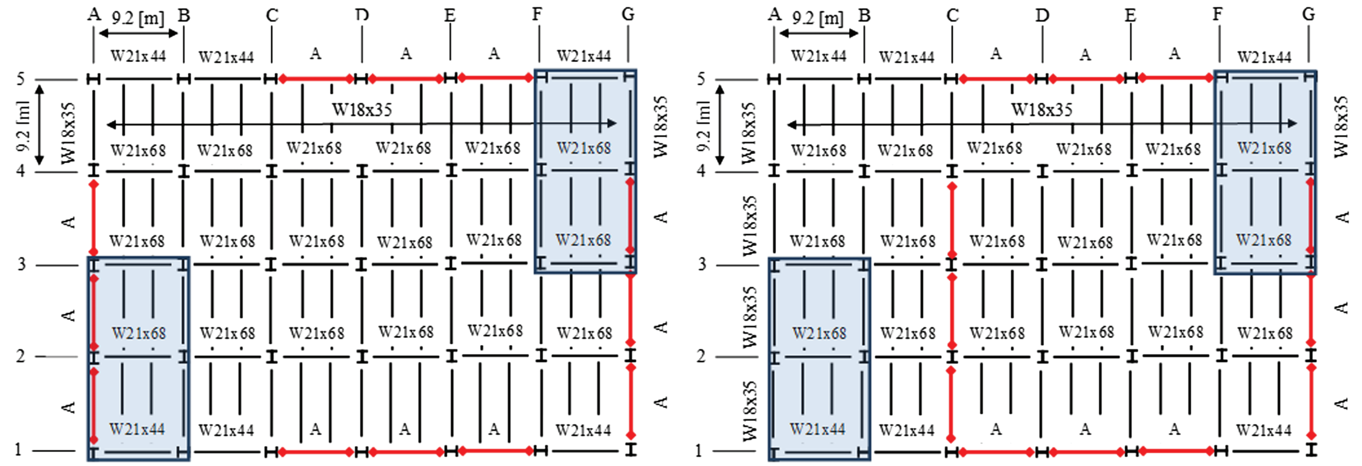

Fig. 3. (Color) (a) Original; (b) altered designs, where locations of staircases are shown in blue and locations of the moment-resisting frames are shown in red

Damage to the Built Environment

The 1994 Northridge, California earthquake with PGA 0.52g and Vs-30 355.8 m/s [PEER Strong Motion Database, File Index 953 (PEER 2013)] was used as the input ground motion for this study. As expected, the two structural configurations produced vastly different responses under this ground motion. For the original structural configuration, there was no noticeable structural damage; the maximum structural responses were relatively small, and well within design tolerances, which is consistent with the findings of Gupta and Krawinkler (2000). For the altered configuration, local collapses occurred in bays on the west side of the structure, destroying the southwest staircase and rendering several offices on the first and second stories impassable. The maximum floor accelerations for the altered configuration increased by nearly an order of magnitude compared to the original configuration. The peak interstory drift ratios increased by nearly two orders of magnitude. The maximum floor accelerations and peak-story drift ratios are provided in Table 2 for the two structural configurations.

Probabilistic damage analysis (Goulet et al. 2007) is used to capture the damage of the nonstructural components that have the largest impact on evacuation time. Focus is placed on suspended ceilings and partition walls because they are frequently damaged in earthquakes and can cause significant delays in the evacuation of building occupants (Phan and Taylor 1996; Meacham et al. 2013). The locations of the partition walls coincide with the locations of all interior walls shown in the floor plans of Fig. 1. Suspended ceilings were assumed to exist in all open interior spaces, including corridors. The fragility functions of Table 3 were used to determine the damage to nonstructural components. Finally the nonstructural and structural damage are translated into new obstacles or areas with reduced evacuation speeds in the environment of the ABM model. An example of the damaged floor plans generated for one simulation for the altered structure is shown in Fig. 4. In the case study, partition walls in damage state D_3 will create an additional impassable area with a thickness of 5.08 cm (2 in.) immediately adjacent to the wall to account for debris caused by the damage. Additionally, it is assumed that walls in damage state D_3 lose any exit signs attached to them, impacting agents that are unfamiliar with the building. Suspended ceilings that fall are assumed to impede foot traffic instead of completely blocking passage. Agents in areas with minor ceiling damage (D_1) experienced no drop in their velocities, but agents in areas with moderate (D_2) and severe (D_3) ceiling damage experienced 10 and 25% drops, respectively, in their maximum speeds. Suspended ceiling damage also will create debris area along with the partition wall at its boundary with a thickness ranging from 5.08 cm (2 in.) for damage state D_1 to 20.32 cm (8 in.) for damage state D_3.

For the original structural configuration, nonstructural damage was generally minor to nonexistent in all the simulations. For the altered configuration, however, damage was significantly more severe. Specific damage rates averaged across all simulations are provided in Table 4.

Table 2. Structural Responses of the Original and Altered Building Configurations

Structural response	Structural configuration	Floor 1	Floor 2	Floor 3
Maximum floor acceleration (g)	Original	0.31	0.35	0.45
	Altered	1.7	2.9	3.4
Peak interstory drift ratio (rad)	Original (10^{-4})	1.28	6.41	6.41
	Altered (10^{-2})	3.08	4.74	3.46

Simulation Results

In this subsection, the results of 20 evacuation scenarios are presented, illustrating the influences of population, social behaviors, and damage levels on evacuation times. In the case study, it is assumed that the evacuation starts at the end of the earthquake and the agents' behaviors during the ground shaking is not considered, though deaths that occurred during the shaking are still included as initial conditions. The agent characteristics used to generate these scenarios are listed in Table 5. For each scenario, the output of the structural analysis is used to conduct 100 MCS to account for the effects of uncertainties in nonstructural damage and human behavior. For each MCS, a new damaged floor plan is generated and the agents are randomly redistributed in the building. The number of simulations was determined such that the ratio of the 99.5% confidence level to the corresponding mean 95% evacuation time is kept within 5% as shown in Table 6; the results were averaged to describe time-varying trends in system behavior.

Three levels of structural damage were used for the evacuation simulations: undamaged, lightly damaged, and heavily damaged. The undamaged structure was included to facilitate comparisons

Table 3. Fragility Functions of Nonstructural Components Used for Damage Assessment (Data from ATC 2012)

Nonstructural component	x	Damage state	x_m	β
Partition walls	Peak interstory drift ratio (rad)	D_1	0.0021	0.6
		D_2	0.0071	0.45
		D_3	0.012	0.45
Suspended ceiling with area <23 m^2	Peak floor acceleration (g)	D_1	1.00	0.4
		D_2	1.80	0.4
		D_3	2.40	0.4
Suspended ceiling with 23 m^2 < area < 93 m^2	Peak floor acceleration (g)	D_1	0.70	0.4
		D_2	1.15	0.4
		D_3	1.80	0.4
Suspended ceiling with 93 m^2 < area < 232 m^2	Peak floor acceleration (g)	D_1	0.45	0.4
		D_2	0.70	0.4
		D_3	1.00	0.4
Suspended ceiling with area >232 m^2	Peak floor acceleration (g)	D_1	0.35	0.4
		D_2	0.55	0.4

Note: Damage states of partition walls are D_1 (screws fall out; minor cracking of wallboard occurs; tape warps or cracks); D_2(moderate cracking or crushing of wallboard occurs, typically in corners and at corners of openings); and D_3(significant cracking or crushing of wallboard occurs; studs buckle; tracks tear). The damage states of suspended ceilings are D_1(5% of tiles dislodge and fall); D_2 (30% of tiles dislodge and fall; t-bar grid is damaged); and D_3 (Ceiling tiles and t-bar grid collapse entirely).

Fig. 4. (Color) Example nonstructural damage for (a) floor one; (b) floor two

to standard evacuation drills reported in the literature. The original (code-conforming) structural configuration was used for the evacuation simulations for the lightly-damaged level, while the altered structural configuration that suffers a local collapse was used for the heavily-damaged level. For each damage level, two occupancy rates were considered to show the effects of overpopulation: an uncrowded, normal population of 259 people and an overpopulation of 450 people. For each combination of damage level and population, various combinations of collective and social behaviors were also simulated, as summarized in the first two columns of Table 6. When no social behaviors are considered, all agents are set to be familiar with the building and evacuate following their habitual routines. When only herding behavior is considered, 10% of agents are assumed not to be familiar with the building so they have to either follow the crowd or randomly find an exit route on their own. When only grouping behavior is considered, agents who are familiar with the building will form groups and evacuate with their group mates. When all social behaviors are considered, the grouping and herding assumptions above hold as well as rescuing behavior, which assumes that healthy agents and those with minor

Table 4. Average Damage Results of Nonstructural Components

Component	Floor	Structural configuration	Damage state D_0 (%)	D_1(%)	D_2(%)	D_3(%)
Partition walls	1	Original	100.00	0.00	0.00	0.00
		Altered	0.00	0.00	0.00	100.0
	2	Original	98.20	1.80	0.00	0.00
		Altered	0.00	0.00	0.00	100.0
	3	Original	97.20	2.80	0.00	0.00
		Altered	0.00	0.00	0.00	100.0
Suspended ceilings	1	Original	98.67	1.21	0.09	0.02
		Altered	7.21	38.04	27.49	27.26
	2	Original	97.67	2.06	0.24	0.04
		Altered	0.33	27.49	17.70	72.82
	3	Original	93.87	5.33	0.67	0.13
		Altered	0.07	27.26	11.78	83.63

Table 5. Variables and Corresponding Values Used in the ABM Evacuation Scenarios

Variables used in evacuation scenarios	Corresponding values
Percentage of agents who are familiar with the building	90% if herding behavior is considered, 100% otherwise
Percentage of familiar of agents who start in their home offices	90%
Vision range	5 m
Mean of altruism constant	0.8
Standard deviation of altruism constant	0.05
Health states	Healthy = 3
	Minor injuries = 2
	Major injuries = 1
	Dead = 0
Minor injury speed reduction	25%
Major injury speed reduction[a]	90%
Space scale	5.08 cm (2 in.)
Time scale	1 s
Patch size	1

[a]The slowest speed of an agent is set as 1 in the model.

Table 6. Statistics of Time to Evacuate 100% of the Building Population for Each Damage Scenario

Damage status	Behaviors included	Time w/population = 259 (s)			Time w/population = 450 (s)		
		Mean	SD	Con.[a]	Mean	SD	Con.[a]
Not damaged	No social behavior	230	13	3	367	22	4
	Herding only	231	15	3	370	21	4
	Grouping only	284	18	3	448	23	4
	All social behavior	281	17	3	439	27	5
Lightly damaged	No social behavior	378	239	47	515	211	42
	Rescuing only	238	43	9	375	31	6
	All social behavior	286	45	9	446	37	7
Heavily damaged	No social behavior	1,286	508	101	1,679	582	116
	Rescuing only	534	444	88	775	444	88
	All social behavior	590	288	57	830	265	52

[a]99.5% confidence level.

injuries may help others they encounter with severe injuries. Additionally, information sharing is included for all scenarios to ensure agents can evacuate successfully.

For the lightly damaged structure, injury rates were based on values reported in ATC-13 for a steel frame low-rise building: agents had 1.2 and 0.16% probabilities of sustaining minor and major injuries, and a 0.04% chance of fatality. Since the non-code-compliant structural system of the heavily damaged building is not included in the construction types listed in ATC-13, injury rates from ATC-13 could not be used directly. Instead, the ATC-13 rates for the code-compliant structure were increased by a factor of 10 (consistent with values of other non code conforming structural types in the same document) to represent the higher risk posed by noncompliant structures. In addition, it is assumed that agents in areas where complete collapses occurred suffered fatal injuries. Agents who perished in the simulation are not rescued by other agents and are left behind.

In each MCS, the total number of agents who exit the building was tracked over time, as was the number of agents who exit from each of the three exterior doors: the main exit, which has large double doors on the south wall that lead to the main lobby; and the northeast and southwest exits, which have smaller fire doors located at the base of the staircases. The flow rates, shown in Table 7, are calculated from the evacuation time histories using the slope of the middle, linear portion of the curves. Additionally, two types of evacuation times were calculated: the time to evacuate all occupants, including the injured, shown in Table 6; and the time to evacuate 95% of the building occupants, shown in Table 8. The mean number of evacuees is plotted with respect to time in Fig. 5 for each damage scenario.

Model Validation

For the undamaged scenarios, the average evacuation rates should agree reasonably well with evacuation drills of similar buildings found in the literature. Hostikka et al. (2007) describe an evacuation drill in which 139 people evacuate from a low-rise office building. This evacuation takes slightly under 6 min. The flow rate from a main door on the first floor in this evacuation is 0.59 persons per second, and the flow rate through a fire door at the base of a staircase is 0.54 persons per second. These flow rates are noted by the authors to be somewhat low, so the overall evacuation times should be considered slightly higher than expected, but these can provide guidance on the expected magnitude for such an evacuation. In another example described by Rinne et al. (2010), the evacuation time is around 4.2 min for 177 people and the flow rates at the exits are

Table 7. Flow Rates (Persons per Second) for Exits by Scenario

Damage status	Behaviors included	Main exit (4 m)		NE exit (1 m)		SW exit (1 m)	
		Population 259	Population 450	Population 259	Population 450	Population 259	Population 450
Not damaged	No social behavior	2.21	3.10	0.51	0.52	0.51	0.52
	Herding only	2.21	3.12	0.51	0.52	0.51	0.52
	Grouping only	1.47	2.02	0.43	0.45	0.43	0.45
	All social behavior	1.47	2.03	0.43	0.45	0.41	0.43
Lightly damaged	No social behavior	2.20	3.13	0.51	0.51	0.49	0.47
	Rescuing only	2.24	3.12	0.51	0.51	0.49	0.50
	All social behavior	1.46	1.99	0.43	0.45	0.41	0.42
Heavily damaged	No social behavior	1.58	2.22	0.50	0.52	N/A	
	Rescuing only	1.58	2.15	0.50	0.52		
	All social behavior	1.02	1.38	0.40	0.43		

Table 8. Mean 95% Evacuation Times for Each Scenario

Damage status	Behaviors included	Time w/population = 259 (s)			Time w/population = 450 (s)		
		Mean	SD	Con.[a]	Mean	SD	Con.[a]
Not damaged	No social behavior	206	12	2	324	21	4
	Herding only	207	14	3	327	21	4
	Grouping only	259	16	3	401	22	4
	All social behavior	256	16	3	390	23	5
Lightly damaged	No social behavior	209	15	3	334	33	7
	Rescuing only	207	14	3	327	20	4
	All social behavior	256	15	3	394	22	4
Heavily damaged	No social behavior	365	36	7	635	77	15
	Rescuing only	356	19	4	583	24	5
	All social behavior	442	26	5	712	96	19

[a]99.5% confidence level.

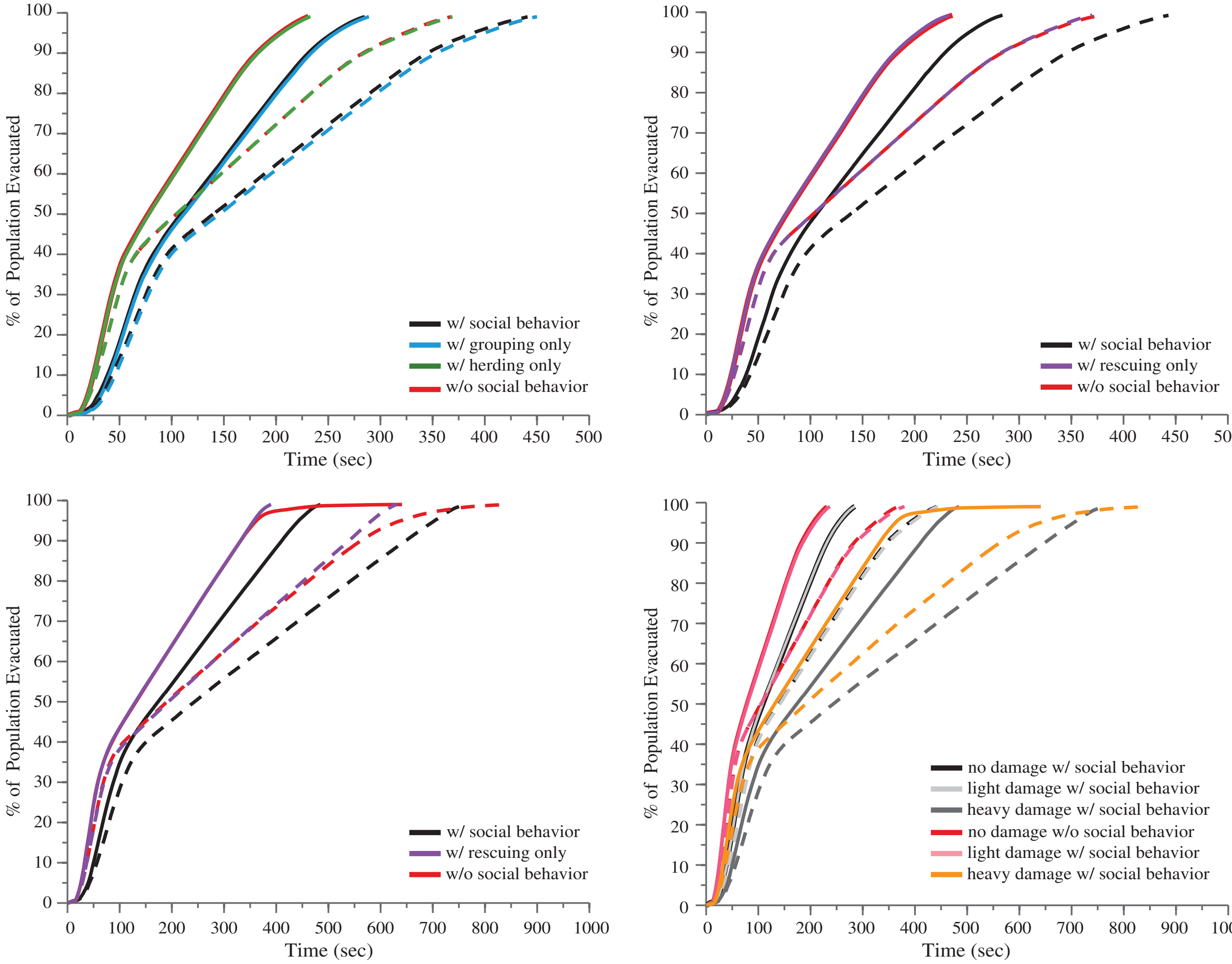

Fig. 5. (Color) Averaged evacuation time history curves for (a) no damage; (b) light damage; (c) heavy damage; (d) all scenarios with and without social behavior; solid lines represent scenarios with 259 occupants and dashed lines represent scenarios with 450 occupants; SB = social behavior

around 0.97 and 1.20 persons per second, repsectively. Therefore, the average evacuation time of 3.78 min without social behavior and 4.65 min with social behavior can be considered reasonable estimates. Adding social behaviors in these simulations provides better estimates when compared to the literature, suggesting that social behaviors play a significant role in evacuation.

The simulation flow rates at the exits are lower than in the discussed literature and the data gathered by Rinne et al. (2010) from 32 events, including fire drills and real events. The trend line introduced by Rinne et al. (2010) as the relationship between the clear door width and the flow rate is given by

$$J = 0.59x + 0.60 \tag{7}$$

where J (persons/s) = flow rate at the door; and x = clear width of a door measured in meters. Although the line doesn't fit the data well and as Gwynne et al. (2009) pointed out that not only the door width but also the doorway mechanisms can affect the flow rates much, the trend line can still be thought to provide a guidance of the average value of the flow rate at a door width. Based on this relationship the flow rates should be around 3 persons per second at the main exit and 1.2 persons per second at the side exits in the model building. Examining the simulation output more closely suggests that the relatively low flow rate at the main exit is actually because the full width of the door is not utilized. In simulations with increased population on the first floor, the flow rate at the main exit increases to ∼3 persons per second with social behavior and ∼4 persons per second without social behavior. The low flow rates at the side exits are because most of people using these exits come from upper floors through relatively narrow staircases that inhibit pedestrian flow. Additional simulations were run to force all agents to evacuate through the side exits. In these simulations, the flow rates are ∼1.2 and ∼1.4 persons per second with social behavior and without social behavior, respectively. These additional results are compared to the empirical relationship of Eq. (7), and are shown to match Rinne et al.'s (2010) results for the exit widths in the case study structure. Therefore, the low flow rates in the case study are impacted by the specific physical characteristics of the building and also population density around an exit.

General Patterns of the Overall Evacuation Time Histories

At the beginning of a simulation, the flow is intermittent, leading to a low average flow rate because only few people with initial locations near an exit will evacuate at this stage. As more people arrive at the exits, the flow rate increases quickly and stabilizes at a constant level as evacuees flow steadily through all the exits. If the building is undamaged and there is only one exit, then the linear portion of the time-history curve will continue until all people have

Nat. Hazards Rev., 2016, 17(1): 04015019

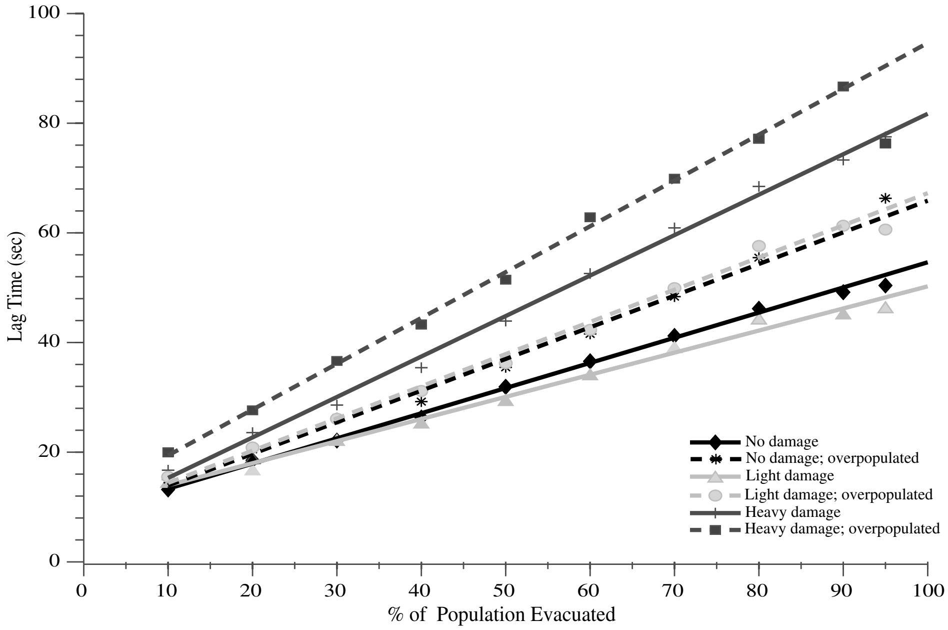

Fig. 6. Lag time (averaged delay time) caused by social behavior versus percent of the population evacuated for all damage scenarios and population cases, with fitted trend lines between data for 10 and 90% population evacuated; $R^2 \geq 0.99$ for all the lines

evacuated. However, if there are multiple exits then the slope of the time history curve will increase until all exits are at their maximum flow capacity and will drop to lower, though still constant, levels as the flows at one or more exits become reduced. These trends are observed even when all exits are identical in size, since variations in the floor plan may cause different numbers of evacuees to choose each exit. Fig. 5(a) demonstrates this trend for the undamaged and lightly-damaged scenarios, for both a population of 259 (solid lines) and a population of 450 (dashed lines). In both of these scenarios, varying numbers of agents choose the main, southwest, and northwest doors. The flow rate drops when all agents who selected the main door have exited, and drops again when all the agents who have selected the southwest door have exited. The first of these drop-offs occurs when roughly 30% of the people have evacuated; the second occurs when roughly 90% of the people have evacuated. The tail end of the time-history curve becomes extended if a small number of badly-injured agents are not rescued and must evacuate on their own. These agents move very slowly, resulting in an extremely long tail at the end of the evacuation time history curve with a slope of nearly zero. Such long evacuation times are far more likely to occur in scenarios that include significant damage but do not include rescuing behavior.

Effects of Social Behaviors, Building Damage, and Population

Effects of Social Behaviors

Grouping behavior will cause delays in the evacuation, as shown in Fig. 5, where solid lines and dashed lines shows scenarios with 259 occupants and 450 occupants, respectively. This is because agents adjust their movement to match the behavior of their social groups and stay close to their group-mates unless they are forced to move forward due to adjacent pedestrain flow. Consequently, a group's speed is lower than the speeds of individuals. It has been observed that grouping behavior also has positive effects, such as cooperation and reduced probability of jamming around exits. Groups can also handle unforseen events better than individuals. However, those behaviors and situations are not yet considered in the model, so the negative effects of the grouping behavior may be exaggerated.

On the other hand, the herding behavior considered in the model helps agents who are unfamiliar with the building layout find a possible evacuation route; it may also exacerbate congestion because exits are not fully utilized. However, the positive effect of herding behavior was more prominent in the simulations of the case study building because only 10% agents in the model are unfamiliar with the building. Therefore, these agents can always can find agents with enough knowledge of the building to inform them of possible evacuation routes without significantly exacerbating congestion. Hence, when only herding behavior is almost equivalent to the scenarios where no social behaviors are considered (and where all agents have complete knowledge of the building). Thus, the averaged time histories for scenarios considering only herding behavior are found to be nearly equivalent to scenarios without social behaviors, as shown in Fig. 5(a).

As expected, rescuing behavior shortens the evacuation time of the injured people, thereby reducing the average and standard deviation of the total evacuation time. Rescuing behavior also reduces the possibility that an injured person blocks evacuation pathways, particularly in the staircases due to their extremely slow pace. However the rescuer and rescuee pair have half the speed of the rescuer, thus, they will obstruct others less even though they will occupy a larger sapce. Fig. 5(c) shows that rescuing behavior has the greatest impact on the final portion of the evacuation event, when over 90% of the occupants have evacuated.

In general, the averaged time-history curves of scenarios with all social behaviors lie to the right of those curves without social behaviors except at the final stages of the evacuations in the severely-damaged scenarios. The distance between the curves with social behavior and those without social behavior can be interpreted as the time lag (delay) caused by the inclusion of social behavior. Fig. 6 shows that the lag time of scenarios including social behaviors increases linearly with the percentage of people evacuated. It also can be seen that severe building damage and overpopulation will increase the lag time. However, this trend reverses in the final stages of evacuations involving injured agents. This is because badly-injured people in scenarios without rescuing social behaviors are more likely to block evacuation pathways. Consequently, the evacuation times of scenarios without social behaviors approaches and eventually exceeds the evacuation times of scenarios with social behaviors. Nevertheless, there are linear trends for the evacuation lag times that are valid throughout most of the time history curves for the damaged building. Specifically, the linear trend is valid up to ∼95% people evacuated for normal population scenarios and up to ∼90% for overoccupied scenarios. For the overpopulated scenarios, there are more badly-injured people; typically, they enter and block staircases only after most of people have evacuated.

The social behaviors decrease the flow rates at the main exit by ∼35% (nearly 1 person per second) and at the side exits by ∼20% (nearly 0.1 persons per second). Again, this decrease is mainly caused by the grouping behavior, where grouping behavior in wide spaces is more significant than in narrow spaces. In narrow spaces, people usually stay closer together due to restriction by obstacles and end up traveling together. Furthermore, the results show that the relative errors of the mean evacuation times due to the consideration of social behaviors are minimized as the evacuation progresses. For example, the relative error continuely drops from around 50 to 60% at the early stage of an evacuation to about 20% at the final stages of evacuation (when ∼95% people have evacuated).

Effects of Building Damage

As expected, building occupants require more time to evacuate from a damaged building than from an undamaged building. The evacuation delays are due to (1) impediments to means of egress, such as the loss of the southwest stairwell in the heavily-damaged scenario; (2) impediments from other physical damage, such as fallen ceiling tiles; and (3) impediments caused by injured occupants blocking evacuation pathways. The time needed to evacuate 95% of the occuapants from the heavily damaged building is nearly double the time required to evacuate the undamaged structure (increase more than 70%). Furthermore, the results show that the impacts of the building damage is greater for a larger population. For instance, for the scenarios with normal population the increment is more than 70% and for the overpopulated scenarios the increment is more than 80%. The evacuation time for 100% of the occupants is increased dramatically if no rescuing behavior is considered, e.g., in the worst case it can be around 30 min.

On the other hand, the flow rates at the side exits are not significantly affected by building damage even when the building is heavily damaged. This is because in all of the scenarios, the staircases leading to the side exits are already fully utilized. However, the flow rate at the main exit decreases by 30% for the heavily-damaged scenarios because of the effects of increases in nonstructural damage and slow-moving injured occupants. The main exit is not fully utilized even in the overpopulated case.

Effects of the Overpopulation

As expected, the overpopulated scenarios have longer mean evacuation times compared to the corresponding normal population scenarios. The 100% evacuation time for the undamaged scenarios increases by ∼60% for the overpopulated cases. The 95% evacuation time for the lightly-damaged and heavily-damaged scenarios also increases by ∼60%. The impact of crowding in buildings is most noticeable for the scenarios where the buiding is heavily damaged and no social behavior is included. In these cases, the 95% evacuation time increases by ∼70%. This can be attributed to the overpopulation, the increase in the total number of injured people, and the impact of nonstructural damage on a greater number of individuals. The flow rates at the side exits does not increase for the overpopulation case because people are queuing in the staircases, even in the normal population case. The flow rate at the main exit, however, increases approximately 40% because the exit is not congested, even in the overpopulated scenarios.

Conclusions

In this paper, an agent-based model is used to simulate the evacuation of individuals from a damaged structure after a seismic event. The physical structure and its damaged state is itself simulated by a fully-dynamic physics-based model coupled with fragility models for nonstructural damage. A heterogenous population is programmed into the model to account for the effects of varying age, gender, body size, speed, and knowledge of building layout on the evacuation process. The agents move with a time resolution of one step per second and are programmed to detect and avoid obstacles, including obstacles arising from structural and nonstructural damage occuring under the seismic event, as well as the movement of people around them. The egress algorithm for the agents includes grouping, herding, rescuing, and the exchange of information with other agents, while maintaining goal-oriented individualistic behaviors of evacuating the building; this is a simplified mathematical model intended to capture the complex crowd behaviors that have been observed during evacuations.

A typical three-story office building was selected as the case study. The simulation results of the undamaged building are compared with fire drills of similar buildings in the literature to validate the agent-based model. Twenty different scenarios were created to study the impacts of social behavior, building damage, and population on total evacuation time. The case study shows that social behaviors play a significant role in the evacuation process. For instance, grouping behavior can result in increased evacuation time. The mean evacuation time of an undamaged building can be underestimated by at least around 20% if social behaviors are ignored. Hence, such behaviors should always be taken into account in engineering-based evacuation models. The case study also showed that in the heavily-damaged building occupants need much more time to evacuate due to both the severe building damage and the injured people, i.e., the time when 95% occupants evacuated are nearly doubled. The results also indicate that a larger population is more susceptible to the building damage. As expected, a larger building population typically takes a longer time to evacuate. In the case study, it is shown that, for the overpopulated scenarios, nearly 60% more time is needed to get 100% of the evacuees out of the undamaged building and to get 95% of the evacuees out of the damaged building.

It is not yet determined whether these results for this single office building can be easily generalized to estimate evacuation patterns of other types of structures. The model is not exhaustive; future iterations of the model should include cooperation among group mates, effects of different doorway mechanisms, and varying the delay time to begin evacuations for all agents. However, this study does present a novel study where detailed engineering tools (e.g., finite-element modeling) are integrated with empirically-based human behavior models to simulate evacuation patterns under realistic damaged conditions, which provides a way to quantify the impacts of the building damage to the evacuation in a single building for a specific ground motion.

While the proposed methods' predictive accuracy has not yet been fully tested, they are useful as a cost-effective simulation tool for social scientists, engineers, and emergency managers for examining a wide range of evacuation scenarios. They can provide insight into the effects of specific adverse situations, such as overpopulation, loss of vertical egress, and vulnerable nonstructural components. These models also provide a test platform for optimizing egress design, including the layout of floor plans to reduce potential jam points and the arrangement of exit signs to promote more-efficient evacuations. Furthermore, the models can be used to improve evacuation procedures in existing structures, and

Nat. Hazards Rev., 2016, 17(1): 04015019

support changes to fire and building codes; more-efficient evacuations are critical in buildings located in tsunami risk zones as well as buildings that may have a risk of collapsing in aftershocks. This single-building framework can also be used to inform larger, community-wide models. The flow rates and evacuation time-histories developed for archetypical buildings in this model can act as input for models of evacuation in large urban areas, where many buildings and building types are present. Such models would play an important role in the study of community resilience.

Acknowledgments

The authors thank Jason Adleberg of Princeton University, Mehdi Jalalpour of Cleveland State University, and Joshua Epstein from the Center for Advanced Modeling at Johns Hopkins University for their early contributions to this work. This work was funded through the Center for Public Health Practice by the Centers for Disease Control and Prevention (cooperative agreement 1P01TP000304-03). Its contents are solely the responsibility of the authors and do not necessarily represent the official views of the Centers for Disease Control and Prevention.

References

AEA-Technology. (2002). "A technical summary of the AEA EGRESS code." *ESRT/NOIL/27812001/002(R)*, Warrington, U.K.

Applied Technology Council. (1985). "Earthquake damage evaluation data for California." *ATC-13 Rep.*, Redwood City, CA.

Applied Technology Council. (2012). "Seismic performance assessment of buildings, 75% complete." *ATC-58 Rep.*, Redwood City, CA.

Badillo-Almaraz, H., Whittaker, A. S., and Reinhorn, A. M. (2007). "Seismic fragility of suspended ceiling systems." *Earthquake Spectra*, 23(1), 21–40.

Beck, J. L., et al. (2002). "Impact of seismic risk on lifetime property values." ⟨http://resolver.caltech.edu/CaltechEERL:2002.EERL-2002-04⟩ (Jan. 1, 2015).

Chu, M. L., Parigi, P., Law, K., and Latombe, J.-C. (2014). "Modeling social behaviors in an evacuation simulator." *Comput. Anim. Virtual Worlds*, 25(3–4), 373–382.

Coburm, A. W., Spence, R. J. S., and Pomonis, A. (1992). "Factors determining human casualty levels in earthquakes: Mortality prediction in building collapse." *Proc., 10th World Conf. on Earthquake Engineering*, A.A. Balkema, Rotterdam, Netherlands, 5989–5994.

Dijkstra, J., Timmermans, H. J. P., and Jessurun, A. J. (2000). "A multi-agent cellular automata system for visualizing simulated pedestrian activity." *Proc., Theoretical and Practical Issues on Cellular Automata*, Cellular Automata for research and Industry, Springer, Berlin, 29–36.

Epstein, J. M. (1996). *Growing artificial societies social science from the bottom up*, Brookings Institution Press, Washington, DC.

Epstein, J. M. (1999). "Agent-based computational models and generative social science." *Complexity*, 4(5), 41–60.

Fiedrich, F., Gehbauer, F., and Rickers, U. (2000). "Optimized resource allocation for emergency response after earthquake disasters." *Saf. Sci.*, 35(1–3), 41–57.

Foley, C. M., Schneeman, C., and Barnes, K. (2008). "Quantifying and enhancing robustness in steel structures. 1—Moment-resisting frames." *Eng. J.*, 45(4), 247.

Fruin, J. J. (1971). *Pedestrian planning and design*, Metropolitan Association of Urban Designers and Environmental Planners, New York.

Galea, E. R., and Perez Galparsoro, J. M. (1994). "A computer-based simulation model for the prediction of evacuation from mass-transport vehicles." *Fire Saf. J.*, 22(4), 341–366.

Galea, E. R., Sharp, G., Lawrence, P., and Dixon, A. J. (2007). "Investigating the impact of occupant response time on computer simulations of the WTC North Tower evacuation." *Proc., 11th Int. Fire Science & Engineering Conf., Interflam 2007*, Vol. 2, Univ. of London, London, 1435–1442.

Goulet, C., et al. (2007). "Evaluation of the seismic performance of a code-conforming reinforced-concrete building—From seismic hazard to loss results," *Earthquake Eng. Struct. Dyn.*, 36(13), 1973–1997.

Gupta, A., and Krawinkler, H. (2000). "Behavior of ductile SMRFs at various seismic hazard levels." *J. Struct. Eng.*, 10.1061/(ASCE)0733-9445(2000)126:1(98), 98–107.

Gwynne, S. M. V. (2013). "Improving the collection and use of human egress data." *Fire Technol.*, 49(1), 83–99.

Gwynne, S. M. V., and Boswell, D. L. (2009). "Pre-evacuation data collected from a mid-rise evacuation exercise." *J. Fire Prot. Eng.*, 19(1), 5–29.

Gwynne, S. M. V., Kuligowski, E. D., Kratchman, J., and Milke, J. A. (2009). "Questioning the linear relationship between doorway width and achievable flow rate." *Fire Saf. J.*, 44(1), 80–87.

Hallquist, J. O. (2006). "LS-DYNA theory manual." Livermore Software Technology Corporation, Livermore, CA.

Helbing, D. (1992). "A fluid-dynamic model for the movement of pedestrians." *Complex Syst.*, 6, 391–415.

Helbing, D., Farkas, I., and Vicsek, T. (2000). "Simulating dynamical features of escape panic." *Nature*, 407, 487–490.

Helbing, D., and Molnar, P. (1995). "Social force for pedestrian dynamics." *Phys. Rev. E*, 51(5), 4282–4286.

Henderson, L. F. (1971). "The statistics of crowd fluids." *Nature*, 229, 381–383.

Horiuchi, S., Murozaki, Y., and Hokugo, A. (1986). "A case study of fire and evacuation in a multi-purpose office building, Osaka, Japan." *Fire Saf. Sci.*, 1, 523–532.

Hostikka, S., Korhonen, T., Paloposki, T., Rinne, T., Matikainen, K., and Heliovaara, S. (2007). "Development and validation of FDS+ EVAC for evacuation simulations project summary report." *VTT TIEDOTTEITA 2421*, VTT, Finland Technical Research Centre of Finland, VTT, Finland.

Hughes, R. L. (2000). "The flow of large crowds of pedestrians." *Math. Comput. Simul.*, 53(4–6), 367–370.

Hughes, T. J. R., and Liu, W. K. (1981a). "Nonlinear finite element analysis of shells. I. Three-dimensional shells." *Comput. Methods Appl. Mech. Eng.*, 26(3), 331–362.

Hughes, T. J. R., and Liu, W. K. (1981b). "Nonlinear finite element analysis of shells. II. Two-dimensional shells." *Comput. Methods Appl. Mech. Eng.*, 27(2), 167–181.

Johnson, C. W. (2005). "Lessons from the evacuation of the world trade centre, 9/11 2001 for the development of computer-based simulations." *Cognition Technol. Work*, 7(4), 214–240.

Khandelwal, K., El-Tawil, S., Kunnath, S., and Lew, H. (2008). "Macromodel-based simulation of progressive collapse: Steel frame structures." *J. Struct. Eng.*, 10.1061/(ASCE)0733-9445(2008)134:7(1070), 1070–1078.

Kirchner, A., and Schadschneider, A. (2002). "Simulation of evacuation processes using a bionics-inspired cellular automaton model for pedestrian dynamics." *Physica A (Amsterdam)*, 312(1–2), 260–276.

Krawinkler, H. (2005). "Van Nuys hotel building Testbed report: Exercising seismic performance assessment." *PEER 2005/11*, Pacific Earthquake Engineering Research Center, Univ. of California, Berkeley, Berkeley, CA.

LAMC (City of Los Angeles Municipal Code). (2013). "Section 9. A1, Building Code. Amended by Ord. No. 182, 850." Los Angeles.

Laufer, Y. (2003). "Age- and gender-related changes in the temporal-spatial characteristics of forwards and backwards gaits." *Physiotherapy Res. Int.*, 8(3), 131–142.

Lim, J., and Krauthammer, T. (2006). "Progressive collapse analyses of 2D steel-framed structures with different connection models." *Eng. J.*, 43(3), 76–201.

Meacham, B., Kim, J. K., and Park, H. (2013). "Structural and nonstructural building system performance during earthquake and post-earthquake fire, fire test program." Dept. of Fire Protection Engineering, Worcester Polytechnic Institute, Worcester, MA.

Mitrani-Reiser, J., and Beck, J. L. (2007). "Incorporating losses due to repair costs, downtime and fatalities in probabilistic-based earthquake engineering." *Proc., ECCOMAS Thematic Conf. on Computational Methods in Structural Dynamics and Earthquake Engineering*, Eccomas, Rethymno, Greece.

Pagni, C. A., and Lowes, L. N. (2006). "Fragility functions for older reinforced concrete beam-column joints." *Earthquake Spectra*, 22(1), 215–238.

Pan, X. (2006). "Computational modeling of human and social behaviors for emergency egress analysis." Ph.D. thesis, Stanford Univ., Stanford, CA.

Peacock, R. D., Averill, J. D., and Kuligowski, E. D. (2010). "Stairwell evacuation from buildings: What we know we don't know." *Pedestrian and evacuation dynamics 2008*, W. W. F. Klingsch, C. Rogsch, A. Schadschneider, and M. Schreckenberg, eds., Springer, Berlin, 55–66.

Peacock, R. D., Averill, J. D., and Kuligowski, E. D. (2013). "Egress from the World Trade Center towers on September 11, 2001." *Fire Technol.*, 49(1), 7–35.

PEER (Pacific Earthquake Engineering Research Center). (2013). "File Index 953." PEER Strong Motion Database, ⟨http://ngawest2.berkeley.edu/⟩ (May 23, 2013).

Pelechano, N., and Malkawi, A. (2008). "Evacuation simulation models: Challenges in modeling high rise building evacuation with cellular automata approaches." *Autom. Constr.*, 17(4), 377–385.

Phan, L. T., and Taylor, A. W. (1996). "State of the art report on seismic design requiements for nonstructural building components." *NISTIR 5857*.

Porter, K., Kennedy, R., and Bachman, R. (2007). "Creating fragility functions for performance-based earthquake engineering." *Earthquake Spectra*, 23(2), 471–489.

Proulx, G., and McQueen, C. (1994). "Evacuation timing in apartment buildings." National Research Council Canada, Ottawa.

Rinne, T., Tillander, K., and Grönberg, P. (2010). "Data collection and analysis of evacuation situations." *VTT Tiedotteita—Research Notes 2562*, 46.

Sadek, F., Main, J. A., Lew, H. S., and Bao, Y. (2011). "Testing and analysis of steel and concrete beam-column assemblies under a column removal scenario." *J. Struct. Eng.*, 10.1061/(ASCE)ST.1943-541X.0000422, 881–892.

Stidwill, D., and Fletcher, R. (2010). *Normal binocular vision: Theory, investigation and practical aspects*, Wiley, Hoboken, NJ.

Still, G. K. (2000). "Crowd dynamics." Ph.D. thesis, Univ. of Warwick, Coventry, U.K.

Wilensky, U. (1999). *NetLogo. V 5.0.4*, Center for Connected Learning and Computer-Based Modeling, Northwestern Univ., Evanston, IL.

Wilensky, U. (2010). "Netlogo, 1999." Center for Connected Learning and Computer-Based Modeling, Northwestern Univ., Evanston, IL.

Zarboutis, N., and Marmaras, N. (2004). "Searching efficient plans for emergency rescue through simulation: The case of a metro fire." *Cognition Technol. Work*, 6(2), 117–126.

Nat. Hazards Rev., 2016, 17(1): 04015019